

## Atomic-resolution observations of semicrystalline intergranular thin films in silicon nitride

A. Ziegler

*Materials Sciences Division, Lawrence Berkeley National Laboratory, Berkeley, California 94720 and Chemistry and Materials Science Directorate, Lawrence Livermore National Laboratory, Livermore, California 94551*

J. C. Idrobo

*Physics Department, University of California, Davis, California 95616*

M. K. Cinibulk

*Materials and Manufacturing Directorate, Air Force Research Laboratory, Wright-Patterson Air Force Base, Ohio 45433*

C. Kisielowski

*National Center for Electron Microscopy, Lawrence Berkeley National Laboratory, Berkeley, California 94720*

N. D. Browning

*National Center for Electron Microscopy, Lawrence Berkeley National Laboratory, Berkeley, California 94720, and Department of Chemical Engineering and Materials Science, University of California, Davis, California 95616*

R. O. Ritchie<sup>a)</sup>

*Materials Sciences Division, Lawrence Berkeley National Laboratory, Berkeley, California 94720 and Department of Materials Science and Engineering, University of California, Berkeley, California 94720*

(Received 17 August 2005; accepted 16 December 2005; published online 27 January 2006)

Nanoscale intergranular films in doped silicon-nitride ceramics are known to markedly affect toughness and creep resistance. They are regarded as being fully amorphous, but are shown here to have a semicrystalline structure in a Ce-doped  $\text{Si}_3\text{N}_4$ . Using two different but complementary high-resolution electron-microscopy methods, the intergranular atomic structure, imaged with sub-angstrom resolution, reveals that segregated cerium ions take very periodic positions, along the intergranular-phase/matrix-grain interface and as a semicrystalline structure spanning the width of the intergranular phase. This result has broad implications for the understanding of the structure and role of the intergranular phase in enhancing the mechanical properties of ceramics. © 2006 American Institute of Physics. [DOI: 10.1063/1.2168021]

Silicon nitrides generally consist of elongated matrix grains that are randomly oriented, interlocked, and separated by nanometer-scale intergranular (IG) films. Their chemical composition and atomic structure are critical to mechanical properties because they control whether the ceramic fractures intergranularly or transgranularly. Such properties can be improved by careful microstructural and compositional design, in particular by controlling the presence and nature of the thin intergranular phases that form in the grain boundaries, invariably due to the presence of rare-earth atoms which are added to aid sintering.<sup>1,2</sup>

For the past three decades, ceramic research has focused on these IG films. Their morphology in  $\text{Si}_3\text{N}_4$  has always been assumed to be amorphous, based on several transmission electron microscopy (TEM) studies<sup>3-5</sup> and thermodynamic calculations.<sup>6,7</sup> Further computational approaches have attempted to model the atomic bonding characteristics by using a variety of interface atom coordination, resulting in predictions for approximate atom positions along the interface between the matrix grain and the intergranular phase.<sup>8-12</sup> However, calculations describing an atomic struc-

ture model that encompasses the entire width of the IG film have been less successful, as essential experimental data about atom positions within the intergranular phase have not been available. Recent studies, however, of the grain-boundary/matrix interface have provided insight into how these IG films are affected by the presence of segregated rare-earth atoms.<sup>13-15</sup> Specifically, each rare-earth element attaches to the interface differently, depending on atomic size, electronic configuration, and the presence of oxygen atoms in the boundary.<sup>14</sup> Calculations indicate that oxygen along grain boundaries in  $\text{Si}_3\text{N}_4$  has a destabilizing effect on the bonding characteristics and serves as a trap for sintering atoms to migrate towards the boundaries.<sup>9</sup> However, due to the preferential attachment to certain interface sites, a partial ordering of the segregated atoms occurs. This is a critical observation as it implies that the IG films in  $\text{Si}_3\text{N}_4$  ceramics are not entirely amorphous, as was previously thought.<sup>3-12</sup>

In this work, we analyze the interface between the grain boundary and crystalline matrix in a high-purity  $\text{Si}_3\text{N}_4$  ceramic, doped with 5 wt%  $\text{CeO}_2$  (and 1 wt%  $\text{Al}_2\text{O}_3$ ), using high-resolution scanning transmission electron microscopy (STEM) and sub-angstrom imaging with phase-contrast, high-resolution transmission electron microscopy (HRTEM). Our objective is to determine how this particular doping el-

<sup>a)</sup> Author to whom correspondence should be addressed; electronic mail: roritchie@lbl.gov

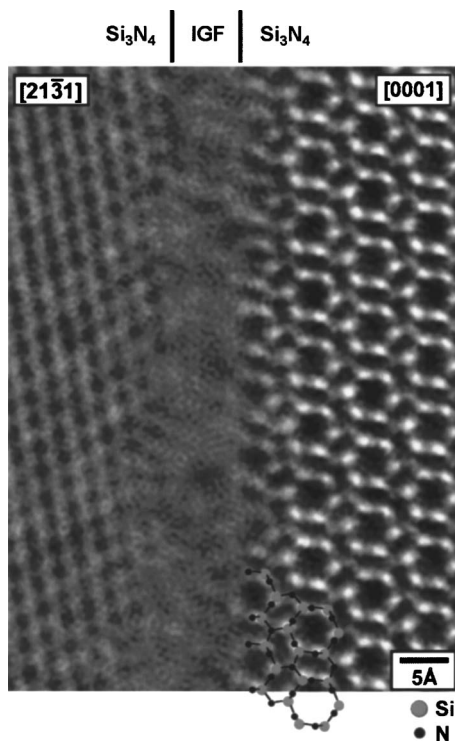


FIG. 1. Phase-reconstructed HRTEM image showing the thin intergranular film (IGF) between two adjacent  $\text{Si}_3\text{N}_4$  grains. The right grain is oriented along the  $[0001]$  crystallographic axis such that individual Si and N atom columns can be discerned in the crystal structure of  $\text{Si}_3\text{N}_4$ . The left grain is misoriented relative to the right grain along  $[31\bar{4}1]$ . The thickness of the intergranular film can be determined from this image to be  $\sim 7\text{--}8$  Å.

ement attaches to the interface, and to determine the extent to which any partial atomic ordering of Ce atoms reaches into the grain-boundary phase.

The Ce-doped  $\text{Si}_3\text{N}_4$  was fabricated via two-step gas-pressure HIP sintering and had a microstructure comprising elongated  $\text{Si}_3\text{N}_4$  matrix grains, with diameters of  $0.2\text{--}1$   $\mu\text{m}$  (aspect ratio  $\sim 15$ ).<sup>16</sup> Phase-contrast microscopy was performed on ground, dimpled and ion-beam milled samples on a 300 kV Philips CM300/FEG/UT microscope. Electron exit waves were reconstructed from a series of 20 lattice images sub-angstrom resolution was achieved via phase retrieval and image reconstruction. STEM imaging was performed with a 200 kV monochromated FEI Tecnai F20 microscope, with a probe size of 0.14 nm. The inner semiangle of the annular dark-field detector was 74 and 110 mrad, with an objective semiangle of 13.5 mrad, conditions that are sufficient to minimize strain-field effects on the Z-contrast image.

HRTEM and STEM images, shown respectively in Figs. 1 and 2, depict the thin intergranular phase between two adjacent  $\beta\text{-Si}_3\text{N}_4$  matrix grains, one of which is oriented along the low-index zone axis  $[0001]$ . The HRTEM image displays a resolution of at least  $0.93$  Å ( $0.093$  nm) such that the position of individual atom columns, including the light nitrogen atom, can be readily discerned in the  $\text{Si}_3\text{N}_4$  crystal structure. With such high resolution, the lattice planes of the opposing matrix grain can be imaged, the crystal orientation was identified as  $[31\bar{4}1]$ , and the thickness of the IG film determined to be  $\sim 7\text{--}8$  Å. The spatial resolution in the STEM image in Fig. 2 is  $1.4$  Å; as this is not sufficient to allow imaging and identification of the opposing matrix grain lattice and its orientation, this matrix grain appears

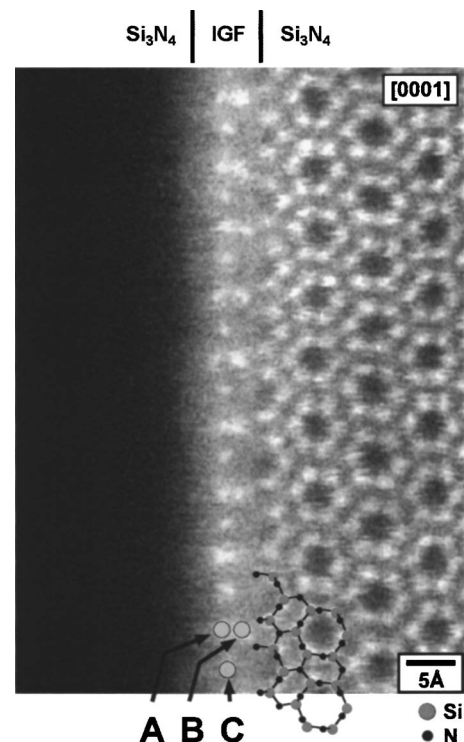


FIG. 2. The corresponding STEM image shows the thin intergranular film (IGF) between the same two adjacent  $\text{Si}_3\text{N}_4$  grains with the same orientations as in the HRTEM image. The spatial resolution obtained with this technique is not as high such that the lattice of the left grain cannot be depicted and it appears dark in the image. However, the Z contrast obtained with this technique reveals the exact positions of the Ce atoms within the intergranular film as bright spots, showing their atomic arrangement and structure, which spans the entire width of the thin intergranular film, connecting both  $\text{Si}_3\text{N}_4$  matrix grains.

dark. However, the Z contrast in the STEM image allows direct identification of the Ce atoms within the thin IG phase. Cerium is a relatively heavy element ( $Z=58$ ) and thus it scatters the incoming electron beam in the microscope more strongly than silicon or nitrogen. Therefore the atomic positions of Ce become visible in the STEM image as bright spots in the IG phase. Note that the positions of these bright spots do not coincide with any atomic position of the  $\text{Si}_3\text{N}_4$  crystal structure. Ce atoms do not substitute for  $\text{Si}_3\text{N}_4$  host atoms in their atomic positions nor do they reside on interstitial sites in the  $\text{Si}_3\text{N}_4$  crystal structure. Ce atoms, as well as other elements, segregate to the IG phase where they can be identified chemically by electron-energy loss spectroscopy.<sup>13–15</sup> As a result, the bright spots in the STEM image represent a distinctly different atomic structure with a periodic arrangement of Ce atoms.

The other sintering aid element Al and the omnipresent Si, N, and O atoms are not resolved in the grain boundary, as their scattering power is less than for Ce and they are most likely not arranged periodically like Si and N in the  $\text{Si}_3\text{N}_4$  crystal structure. A rather random, amorphous-like positioning of any atom in the boundary cannot be imaged due to the random electron scattering processes in the sample, which is another strong indication that the observed Ce atoms are indeed arranged as a crystalline-like structure in the thin grain-boundary films in this material. The entirely new information gathered with these high-resolution images is that the IG films are not completely amorphous and that Ce atoms order across the entire width of the film, essentially

connecting both grains. This is contrary to most previous beliefs. Indeed, a previous study of this same material, using microdiffraction and diffuse dark-field imaging, concluded that the intergranular phase did not show signs of crystalline or semicrystalline structure;<sup>16</sup> however, no direct imaging at the atomic level was possible at that time. The present results represent a crucial new input for atomic structure calculations to assess the strength and the atomic bonding characteristics of the intergranular phase.

It is of note that a recent study<sup>14</sup> on the matrix-grain/IG-film interface has shown how rare-earth atoms attach and bond to the matrix grains depending on atom size and electronic configuration. Sm atoms, for example, arrange in single-atom periodic configuration at two distinct positions along the interface, whereas the larger La atoms do not attach in any periodic form to the interface. The present results on Ce fit well the parameters established in this prior work. Cerium, with atomic number  $N=58$  and a valence shell radius of  $r=2.169$  Å, is slightly heavier and smaller than La ( $N=57$ ,  $r=2.201$  Å), but it is lighter and larger than Sm ( $N=62$ ,  $r=2.164$  Å). According to the atom-size dependence, the distance between the matrix grains and the Ce atoms becomes larger than established for Sm atoms. The arrangement of the Ce atoms, shown in Fig. 2, involves three distinct atomic positions, A, B and C, which form a triangle. The positions A and B are relatively close together and can be regarded as atom pairs with an average separation of  $1.81\pm 0.2$  Å. The A-B atom pair axis is oriented perpendicular to the interface and attaches to the  $\text{Si}_3\text{N}_4$  prism plane in periodic intervals of  $7.08\pm 0.1$  Å. Position C has a single-atom character, and is located between the periodic A-B atom pairs and opposite the open hexagonal rings of the  $\text{Si}_3\text{N}_4$  prism plane. The average distance A-C and B-C is  $3.39\pm 0.15$  and  $3.54\pm 0.18$  Å, respectively. These values compare well with crystallographic data for Ce nitride and oxide structures,<sup>17–19</sup> although the measured A-B separation is significantly smaller than in any of these structures. As the STEM images are a two-dimensional projection of a three-dimensional structure, atom positions A and B are likely shifted relative to each other along (0001).

Although the opposing matrix grain is not visible in the STEM due to insufficient spatial resolution, by determining the IG-film thickness from the concomitant HRTEM image, the interface between the film and the opposing matrix grain can be located in the STEM image. This indicates an extended Ce-atom arrangement spanning the entire width of the IG film, with an invariable connection to the opposing matrix grain.

Finally, we note that for a direct overlay to the STEM image of any Ce-based structure, or single unit cell of it, the simple geometric constraints imposed by the film thickness ( $\sim 7$ – $8$  Å) must be considered. There are a variety of structural options depending on what the Ce atoms are bonded to: N, O, Si or a combination thereof. Additionally, the different positions A, B, and C could possibly be associated with the different valence states that Ce atoms can take, i.e., +3 and +4. However, since known Ce-based unit cells vary between 3.89 Å ( $\text{CeN}_2$ ,  $\text{Ce}_2\text{O}_3$ ) in their shortest and 13.056 Å ( $\text{Ce}_2\text{Si}_2\text{O}_7$ ) in the longest dimension, making them difficult to fit as set unit cells in the boundary space, a probable way of constructing the boundary Ce-based crystalline structure is by using only the basic building blocks of these unit cells,

e.g., the common tetrahedral structure. One possible design is that Ce-based tetrahedra are ordered along the IG film following the periodicity of the observed Ce-atom arrangements. The restricted grain-boundary space and required high Ce–O coordination number (6–9) is unlikely to limit the structural possibilities. The distance between a Ce ion and the surrounding O (N) ions is of the order of 1 Å. Specifically, the effective ionic radius increases for a  $\text{Ce}^{3+}$  ion from 1.034 to 1.14 Å when the coordination number increases from 6 to 8; on the other hand, the effective ionic radius decreases considerably from 1.034 to 0.8 Å when the electronic configuration changes from  $\text{Ce}^{+3}$  to  $\text{Ce}^{+4}$  for a sixfold coordinated Ce ion.<sup>19</sup> Additionally, between the simple  $\text{CeO}$ ,  $\text{CeN}$  and the rather complex  $\text{Ce}_2\text{Si}_2\text{O}_7$  structures are many other structural variations with a range of Ce–O(N) separations and tetrahedral-type substructures, such that forming a Ce-based crystalline structure that fits the structural data obtained in the STEM images should be feasible.

The experimental fact is that the Ce ions are located at very specific atomic positions along the grain boundary, as seen in the current STEM images, and since this is observed on a real material, there is no doubt that a Ce-based periodic structure exists along the thin grain boundaries in  $\text{Si}_3\text{N}_4$ . The precise grain-boundary structure is as yet unknown and will require further experimental and particularly computational studies, although ordering of the intergranular phase has been predicted in MD calculations.<sup>20–22</sup>

This work was supported by the Director, Office of Science, Office of Basic Energy Sciences, Division of Materials Sciences and Engineering, of the U.S. Department of Energy under Contract Nos. DE-AC02-05CH11231 and DE AC05-03ER46057.

<sup>1</sup>P. F. Becher, S. L. Hwang, and C. H. Hsueh, *MRS Bull.* **20**, 23 (1995).

<sup>2</sup>S. M. Wiederhorn, *Annu. Rev. Mater. Sci.* **14**, 373 (1984).

<sup>3</sup>H. J. Kleebe, J. Bruley, and M. Rühle, *J. Eur. Ceram. Soc.* **14**, 1 (1994).

<sup>4</sup>H. J. Kleebe, M. J. Hoffmann, and M. Rühle, *Z. Metallkd.* **83**, 610 (1992).

<sup>5</sup>H. J. Kleebe, M. K. Cinibulk, I. Tanaka, J. Bruley, R. M. Cannon, D. R. Clarke, M. J. Hoffmann, and M. Rühle, *Mater. Res. Soc. Symp. Proc.* **287**, 65 (1993).

<sup>6</sup>D. R. Clarke, *J. Am. Ceram. Soc.* **70**, 15 (1987).

<sup>7</sup>D. R. Clarke, T. M. Shaw, A. P. Philipse, and R. G. Horn, *J. Am. Ceram. Soc.* **76**, 1201 (1993).

<sup>8</sup>P. Dudesek and P. L. Benco, *J. Am. Ceram. Soc.* **81**, 1248 (1998).

<sup>9</sup>L. Benco, *Surf. Sci.* **327**, 274 (1995).

<sup>10</sup>T. Nakayasu, T. Yamada, I. Tanaka, H. Adachi, and S. Goto, *J. Am. Ceram. Soc.* **81**, 565 (1998).

<sup>11</sup>P. Rulis, J. Chen, L. Ouyang, W.-Y. Ching, X. Su, and S. H. Garofalini, *Phys. Rev. B* **71**, 235317 (2005).

<sup>12</sup>M. Yoshiya, I. Tanaka, and H. Adachi, *Acta Mater.* **48**, 4641 (2000).

<sup>13</sup>N. Shibata, S. J. Pennycook, T. R. Gosnell, G. S. Painter, W. A. Shelton, and P. F. Becher, *Nature (London)* **428**, 730 (2004).

<sup>14</sup>A. Ziegler, J. C. Idrobo, M. K. Cinibulk, C. Kisielowski, N. D. Browning, and R. O. Ritchie, *Science* **306**, 1768 (2004).

<sup>15</sup>G. B. Winkelman, C. Dwyer, T. S. Hudson, D. Nguyen-Mahn, M. Dobliger, R. L. Satet, M. J. Hoffmann, and D. J. H. Cockayne, *Philos. Mag. Lett.* **84**, 755 (2004).

<sup>16</sup>H. J. Kleebe and M. K. Cinibulk, *J. Mater. Sci. Lett.* **12**, 70 (1993).

<sup>17</sup>H. Bäringhausen and G. Schiller, *J. Less-Common Met.* **110**, 385 (1985).

<sup>18</sup>D. J. M. Bevan, *J. Inorg. Nucl. Chem.* **1**, 49 (1955).

<sup>19</sup>R. D. Shannon and C. T. Prewitt, *Acta Crystallogr., Sect. B: Struct. Crystallogr. Cryst. Chem.* **B25**, 925 (1969).

<sup>20</sup>S. H. Garofalini and W. Luo, *J. Am. Ceram. Soc.* **86**, 1741 (2003).

<sup>21</sup>X. Su and S. H. Garofalini, *J. Mater. Res.* **19**, 752 (2004).

<sup>22</sup>X. Su and S. H. Garofalini, *J. Mater. Res.* **19**, 3679 (2004).